

Supporting information for

Thiol functionalized covalent organic frameworks for highly selective enrichment and detection of mercury by matrix-assisted laser desorption/ionization time-of-flight mass spectrometry

Qianqian Sun^a, Wende Ma^a, Dan Ouyang^a, Guorong Li^a, Yixin Yang^a, Xi Yan^a, Hang Su^a, Zian Lin^{a,*}, and Zongwei Cai^{b,*}

a. Ministry of Education Key Laboratory of Analytical Science for Food Safety and Biology, Fujian Provincial Key Laboratory of Analysis and Detection Technology for Food Safety, College of Chemistry, Fuzhou University, Fuzhou, Fujian, 350108, China

b. State Key Laboratory of Environmental and Biological Analysis, Department of Chemistry, Hong Kong Baptist University, 224 Waterloo Road, Kowloon Tong, 999077, Hong Kong, SAR, P. R. China

- **First corresponding author:** Zian Lin;
- **Second corresponding author:** Zongwei Cai;
- **Postal address:** College of Chemistry, Fuzhou University, Fuzhou, Fujian 350108, China
- **Fax:** 86-591-22866135

E-mail: zianlin@fzu.edu.cn (Z. Lin); zwcai@hkbu.edu.hk (Z. Cai)

Materials and reagents. 1,3,5-tris(4-aminophenyl) benzene (Tab) and 2,5-bis(2-propyn-1-yloxy)-1,4-benzenedicarboxaldehyde (BTP) were purchased from Jilin Chinese Academy of Sciences-Yanshen Technology Co. Ltd. (Jilin, China). Pentaerythritol tetra (3-mercaptopropionate) were purchased from Aladdin Chemistry Co. Ltd. (Shanghai, China). 4-mercaptopbenzoic acid was obtained from Tokyo Chemical Industry. (Tokyo, Japan). All metal solutions and solvents were of analytical grade.

Characterization. The structure and composition of the alkynyl-terminated COFs and COFs-SH materials were characterized by scanning electron microscopy (SEM; Nova NanoSEM 230, FEI Czech Republic S.R.O, Czech Republic), transmission electron microscopy (TEM; TECNAI G2 F20, FEI, USA), powder X-ray diffraction (PXRD; DY5261/Xpert3, CEM, USA), N₂ adsorption and desorption (ASAP 2020, Micromeritics, USA), X-ray photoelectron spectroscopy (XPS; ESCALAB 250, VG, USA), nuclear magnetic resonance spectrometer (NMR; AVANCE III 500, Bruker, Switzerland), Fourier transform infrared (FT-IR) spectra (AVATAR360, Thermo, USA), element analysis (Vario EL Cube, elementar, Germany).

Adsorption kinetic models

The pseudo-first order and pseudo-second order kinetics models were expressed as follow:

pseudo-first-order kinetics: $\log(Q_e - Q_t) = \log Q_e - K_1 t / 2.303$

pseudo-second-order kinetics: $t/Q_t = t/Q_e + 1/K_2 Q_e^2$

where Q_t (mg/g) is the amount of Hg^{2+} adsorbed at time t (min), Q_e (mg/g) is the amount of Hg^{2+} adsorbed at equilibrium, K_1 (min^{-1}) and K_2 ($g\ mg^{-1}min^{-1}$) is represented as the rate constant for pseudo-first-order kinetics pseudo-second-order kinetics.

Adsorption isothermal models

To further evaluate the maximum adsorption capacity of COFs-SH, other adsorption isothermal models, including the Freundlich, and the Temkin models, were employed.

The expressions were given as follow:

Freundlich model: $\ln Q_e = \ln K_F + \ln C_e/n$

Temkin: $Q_e = B \ln a_T + B \ln C_e$

where the Freundlich constant and $1/n$ is the intensity of adsorption, a_T is the equilibrium gas constant, B is the correlation constant of Temkin model.

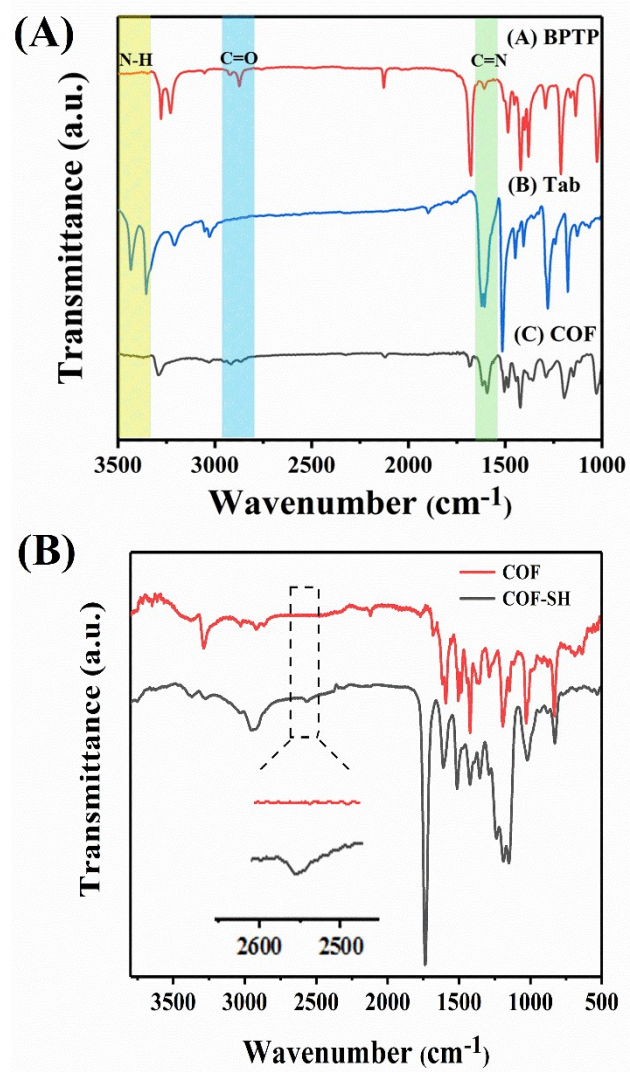


Fig. S1. (A) FT-IR spectra of alkyne-terminated COFs and corresponding monomers;

(B) FT-IR spectra of alkyne-terminated COFs and COFs-SH;

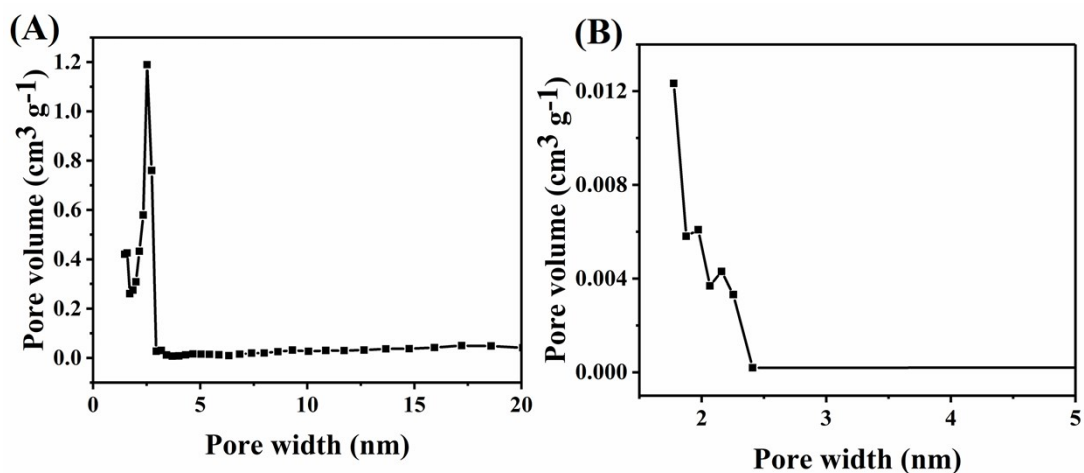


Figure S2. Pore size distribution of (A) alkynyl-terminated COFs and (B) COFs-SH.

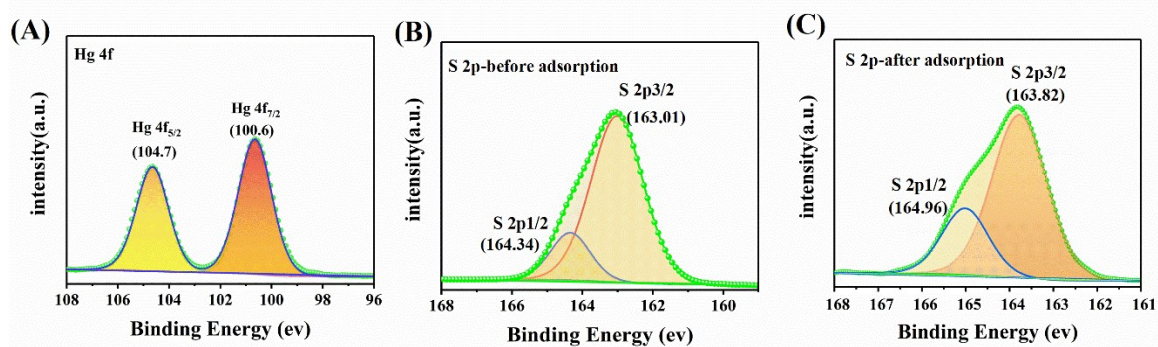


Figure S3. The XPS spectra of (A) Hg 4f; (B) S 2p (before adsorption with COFs-SH); (C) S 2p (after adsorption with COFs-SH).

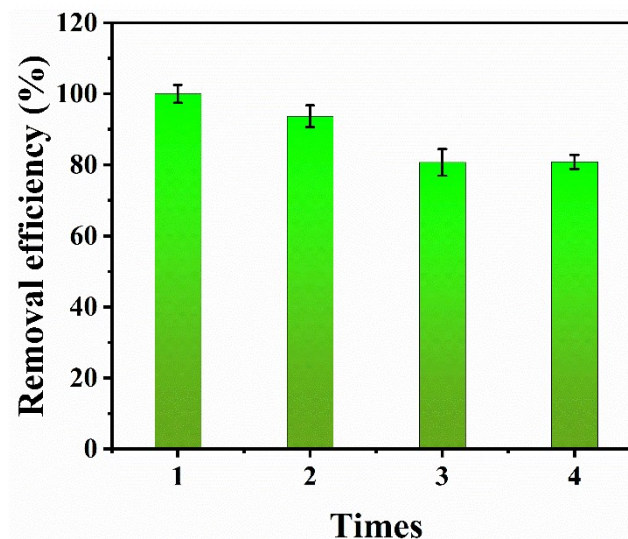


Fig. S4. Reusability of COFs-SH for the adsorption of Hg²⁺.

Table S1. The elemental analysis of N, C, H, S of COFs-SH.

Sample	N (%)	C (%)	H (%)	S (%)
□	3.00	57.07	4.69	11.36

Table S2. Kinetic parameters for Hg²⁺ adsorption.

Model	Qm (mg/g), cal	K	Qm (mg/g), exp	R ²
Pseudo-first-order	70.87	0.044	572.43	0.9164
Pseudo-second-order	574.71	0.002	572.43	0.9998

Table S3. Adsorption isotherms parameters for Hg²⁺ adsorption.

Adsorption isothermal models	parameters	Hg ²⁺
Freundlich model	K _F	16.86
	n	14.54
	R ²	0.962
Temkin model	a _T	35.17
	B	37.93
	R ²	0.970

Table S4. The reproducibility of the analysis of Hg²⁺ with the developed method.

Analytes	shot-to-shot RSD (n=3)[a]	sample-to-sample RSD (n=3)[b]	LOD (pg/mL)
Hg ²⁺	4.5%	4.7%	80

[a] The shot-to-shot RSDs were measured based on 3 shots at different locations on the matrix.

[b] The sample-to-sample RSDs were measured based on 3 samples in different batches.

Table S5. Comparison of the current work with the other references.

Analysis technology	Materials	LODs	References
fluorometric detection	BODIPY	0.37 μM	[45]
electrochemical detection	pS-rGO	0.5 nM	[46]
fluorescence detection	CQDs	12.43 nM	[47]
ICP-OES	MGO	0.05 $\mu\text{g/L}$	[48]
electrochemical sensor	Zr-DMBD MOFs/3D-KSC	0.05 μM	[49]
MALDI-TOF-MS	Thymine chitosan nanomagnets	0.05 nM	[50]
MALDI-TOF-MS	COFs-SH	80 pg/mL (equal to 396 $\text{amol}/\mu\text{L}$)	This work